

Exploring Conventional Approaches for Color Image Denoising: A Comparative Study

Nagasubhadra D. Uppalapati^{1*}, Praveen B. Choppala²

^{1*}Dept. of E.C.E., Andhra University, Email:subhadrauppalapati@gmail.com

²Dept. of E.C.E. WISTM, Andhra University, Email: praveenbchoppala@gmail.com

Abstract: Image denoising plays a critical role in enhancing the quality of digital images by removing unwanted noise while preserving important image details. Among various noise types, color image denoising presents unique challenges due to the complex correlation between color channels. This paper explores conventional denoising approaches specifically tailored for color images, focusing on well-established techniques such as median filtering, Gaussian smoothing, bilateral filtering, Non-Local Means (NLM), and wavelet-based denoising. Each method is analyzed for its effectiveness in suppressing noise while maintaining image integrity. We perform a comparative study to evaluate the performance of these techniques across different noise models, including Gaussian, salt-and-pepper, and speckle noise. Objective metrics such as Peak Signal-to-Noise Ratio (PSNR) and Root Mean Square Error (RMSE) are used to assess image quality post-denoising. Our results highlight the strengths and limitations of each method, offering insights into which conventional approaches are most suitable for specific noise types and image content. This comparative analysis serves as a foundation for further research and development of advanced denoising techniques.

Keywords: Impulse Noise, Color Image Restoration, Median Filtering, Bilateral Filtering, Non-Local Means (NLM), Image Quality Assessment (PSNR, SSIM).

1. Introduction

Image denoising is a fundamental problem in the field of image processing and computer vision, where the objective is to remove noise from an image while preserving its important details. The presence of noise, whether introduced during image acquisition, transmission, or storage, can degrade the visual quality and hamper subsequent processing tasks like segmentation, recognition, and compression. Denoising becomes particularly challenging in color images, as there is an intricate correlation between the three-color channels (Red, Green, and Blue), and improper handling can result in color artifacts or loss of details [1,2].

Over the years, numerous denoising techniques have been developed, ranging from simple filtering operations to more advanced approaches. Conventional methods, which form the backbone of early denoising efforts, continue to serve as benchmarks for evaluating modern algorithms [3]. These methods include spatial domain techniques such as median filtering, Gaussian smoothing, and bilateral filtering, as well as frequency domain approaches like wavelet-based denoising [4-8]. Each of these techniques offers distinct advantages and drawbacks depending on the nature of the noise and image content. For instance, while median filtering is highly effective in reducing impulse noise (salt-and-pepper noise), it may blur fine details. Gaussian smoothing is suitable for Gaussian noise but may not perform well for other types of noise, such as speckle or impulse noise. In addition to spatial and frequency domain methods, more advanced approaches such as Non-Local Means (NLM) filtering have gained significant attention for their ability to exploit redundancy in image structures. NLM filtering has proven particularly effective in reducing noise while

preserving details by averaging similar patches in an image, rather than just pixels in the local neighborhood [9-12].

In this paper, we conduct a comprehensive comparative study of these conventional denoising methods, focusing on their performance in removing various types of noise, including Gaussian noise, salt-and-pepper noise, and speckle noise, from color images. Using widely accepted objective metrics such as Peak Signal-to-Noise Ratio (PSNR) and Structural Similarity Index (SSIM), we evaluate the efficacy of each approach in terms of noise suppression and detail preservation. Our study aims to provide insights into the suitability of different conventional techniques for color image denoising, guiding researchers and practitioners in selecting the appropriate method for specific noise scenarios [13-14]. This comparative analysis not only highlights the strengths and weaknesses of traditional methods but also sets the stage for future research into more advanced and hybrid techniques, as well as their potential applications in real-world scenarios where image quality is paramount.

The rest of the paper is organized as follows: Section 2 describes different types of noise and their mathematical models, providing a detailed understanding of the various noise characteristics encountered in color images. Section 3 reviews conventional denoising methods, including their principles and applications for mitigating different noise types. Section 4 presents a comprehensive study of these denoising methods, comparing their effectiveness and performance in practical scenarios. Finally, Section 5 concludes the paper, summarizing the findings and offering insights into future research directions.

2. Noise Models

Noise in color images refers to unwanted variations or distortions in pixel values, often introduced during image acquisition, transmission, or compression. In mathematical terms, noise is typically modeled as a random process added to the original signal (image). Below is an overview of common types of noise in color images and their corresponding mathematical representations.

2.1. Gaussian Noise

Gaussian noise is one of the most common noise types in images and is usually caused by sensor imperfections, heat, or other environmental conditions [2]. It is modeled as independent, identically distributed random variables with a normal distribution.

Let the observed noisy pixel $X(i, j, c)$ at position (i, j) in a color channel c where $c \in \{R, G, B\}$ $i = 1, 2, \dots, M$ and $j = 1, 2, \dots, N$. M represents number of rows and N represents number of columns as:

$$Y(i, j, c) = X(i, j, c) + N(i, j, c) \quad (1)$$

$X(i, j, c)$ is the original pixel value, $N(i, j, c) \sim \mathcal{N}(0, \sigma^2)$ is Gaussian noise, where $\mathcal{N}(0, \sigma^2)$ represents a normal distribution with mean typically assumed for zero-mean Gaussian noise and variance σ^2 controls the noise intensity. Each pixel in the image has noise added from the Gaussian distribution independently, and this noise affects each color channel (Red, Green, Blue) independently or collectively. The probability density function (PDF) for Gaussian noise is

$$p(N) = \frac{1}{\sqrt{2\pi\sigma^2}} \exp\left(-\frac{N^2}{2\sigma^2}\right) \quad (2)$$

2.2 Speckle Noise (Multiplicative Noise)

Speckle noise is often found in images obtained via coherent imaging systems, such as radar, ultrasound, and synthetic aperture radar (SAR) [15]. It is multiplicative, meaning the noise intensity is proportional to the pixel value.

$$Y(i, j, c) = X(i, j, c) \times N(i, j, c) \quad (3)$$

$N(i, j, c)$ is multiplicative noise, often modeled as a random variable with a gamma distribution $N(i, j, C) \sim \text{Gamma}(\alpha, \beta)$ (4)

where α and β are shape and scale parameters, respectively. Increases with pixel intensity, making bright regions more affected than darker ones. It is common in medical and remote sensing images. Requires specialized denoising techniques such as wavelet or homomorphic filtering to handle this multiplicative nature.

2.3 Poisson Noise (Shot Noise)

Poisson noise, or shot noise, is commonly observed in photon-limited imaging systems, such as low-light photography or medical imaging [16]. It arises from the quantization of image signals, where the number of photons detected by a sensor follows a Poisson distribution. For each pixel, the observed intensity is modeled as

$$Y(i, j, c) \square \text{Poisson}(X(i, j, c)) \quad (5)$$

Where $\text{Poisson}(\lambda)$ is the Poisson distribution with parameter $\lambda = (X(i, j, c))$, representing the mean and variance of the distribution. Noise variance is proportional to the pixel intensity, with brighter regions having higher variance. Poisson noise often observed in low-light conditions or high-sensitivity cameras. Non-Gaussian, making standard filtering techniques less effective.

2.4 Uniform Noise

Uniform noise is less common but can arise from quantization errors or uniform random fluctuations during image acquisition [17]. Uniform noise is modeled as

$$Y(i, j, c) = X(i, j, c) + N(i, j, c) \quad (6)$$

Where $N(i, j, c) \sim U(a, b)$ a uniform distribution with bounds a and b . The noise values are distributed uniformly within the range $[a, b]$. Uniform noise generally simpler to handle due to its uniform nature, making basic filters effective in removing this noise. The probability density function for uniform noise is

$$p(N) = \frac{1}{b-a}, N \in [a, b] \quad (7)$$

2.5 Salt-and-Pepper Noise (Impulse Noise)

Salt-and-pepper noise, also known as impulse noise, typically appears as randomly occurring white and black pixels in the image, representing extreme pixel values (minimum and maximum) [18]. It is common in scenarios with sharp signal disturbances or transmission errors.

Let us considering $x_{i,j}, i = 1, 2, \dots, M, j = 1, 2, \dots, N$ containing MN pixels, with originally unsigned integers in the interval $(0, 255)$, to be scaled as real values in the interval $(0, 1)$ so that a zero represents the lowest intensity and a one represents the highest.

Let $Z = (z_{i,j}, i = 1, \dots, M, j = 1, \dots, N)$ be the image corrupted by impulse noise. As discussed earlier, impulse noise is mainly classified in to two types, fixed valued impulse noise (a.k.a. salt and pepper noise) and random valued impulse noise. In the fixed valued impulse noise, a pixel is corrupted with probability $p \in (0, 1)$. A corrupted pixel implies that one of its red, green, or blue components gets corrupted by a railing to 0 (full black) or 255 (full white) with uniform probability across the color components.

One standard formulation of the Fixed Valued Impulse Noise is where a pixel is considered to be noisy with probability and all three-color channels in that noisy pixel predicted to be either one or zero with equal probability represented as

$$z_{i,j} = \begin{cases} x_{i,j} & \text{if } q \geq p \\ (0,0,0) & \text{if } q < p, r \geq \frac{1}{2} \\ (1,1,1) & \text{if } q < p, r < \frac{1}{2} \end{cases} \quad (8)$$

The formulation of the Random Valued Impulse Noise model is described as

$$z_{i,j} = \begin{cases} x_{i,j} & \text{if } q \geq p \\ (x_{i,j,r}, x_{i,j,g}, a) & \text{if } q < p, r < \frac{1}{3} \\ (x_{i,j,r}, a, x_{i,j,b}) & \text{if } q < p, \frac{1}{3} \leq r < \frac{2}{3} \\ (a, x_{i,j,g}, x_{i,j,b}) & \text{if } q < p, \frac{2}{3} \leq r \end{cases} \quad (9)$$

where $a = \begin{cases} 1 & \text{if } s \geq 0.5, s \in (1,0) \\ 0 & \text{otherwise} \end{cases}$

Impulse noise, such as salt-and-pepper noise, appears as random black and white pixels in an image, often caused by transmission errors or sensor faults. It is more difficult to remove because it affects only a few isolated pixels while leaving others intact, making it challenging to distinguish between noise and fine details. Conventional filters may blur important image structures while attempting to remove the noise. Additionally, its random occurrence complicates the denoising process without losing significant image features.

3. Conventional Methods

Conventional methods like median filtering, Gaussian smoothing, bilateral filtering, and wavelet-based denoising each offer unique strengths and weaknesses, making them suitable for different types of noise and image content. The choice of technique depends heavily on the noise characteristics and the application requirements, with more advanced techniques like Non-Local Means and modern hybrid approaches offering improved performance in complex scenarios. Over time, image denoising has evolved significantly, beginning with relatively simple methods and advancing to more sophisticated algorithms. Simple methods, such as linear filtering, were among the first to be applied in image denoising. However, these methods often suffer from limitations, such as blurring edges and fine details, which led to the development of more advanced techniques. Conventional methods remain relevant as they offer insights into the behavior of noise and image structures,

providing benchmarks for more modern and complex algorithms.

3.1. Spatial Domain Techniques

Mean filtering: Mean Filtering works by replacing the value of each pixel in an image with the average value of its neighboring pixels. This process smooths the image and helps in reducing noise, particularly in images with Gaussian noise. It's one of the simplest types of spatial filters.

$$Y(i, j) = \frac{1}{N} \sum_{(m,n) \in W(i,j)} X(i, j) \quad (10)$$

Where $X(i, j)$ is the original image, $Y(i, j)$ is the filtered image, (m, n) is the window centered at (i, j) , and N is the number of pixels in (i, j) .

Median Filtering: Median filtering is a non-linear technique that replaces each pixel value with the median of its surrounding neighbors. It is particularly effective in handling impulse noise, such as salt-and-pepper noise, where individual pixels may take extreme values. Median filtering can remove these noisy pixels while preserving the overall structure of the image. However, one major drawback is that it may also remove fine details in the image, especially if the filter window size is too large. As a result, textures and small image features can be lost, leading to over smoothing.

$$Y(i, j) = \text{Median}\{X(m, n) \mid (m, n) \in w(i, j)\} \quad (11)$$

where $\text{Median}\{\dots\}$ denotes the median value within the window $W(i, j)$.

Gaussian Smoothing: Gaussian smoothing is a linear filter that applies a Gaussian kernel to average the intensity values of surrounding pixels. This method is highly effective at removing Gaussian noise, which is a common type of noise characterized by a normal distribution. The Gaussian filter's strength lies in its simplicity and efficiency. However, one of its main limitations is its tendency to blur edges, as it does not discriminate between noise and important image structures like sharp edges. Additionally, Gaussian smoothing is not particularly effective for non-Gaussian noise types, such as speckle noise or impulse noise, which may require more specialized filters.

$$Y(i, j) = \sum_{(m,n) \in W(i,j)} X(i, j).G(i-m, j-n) \quad (12)$$

where $G(i, j)$ is the Gaussian kernel defined by

$$G(i, j) = \frac{1}{2\pi\sigma^2} \exp\left(-\frac{i^2 + j^2}{2\sigma^2}\right) \quad (13)$$

where σ is the standard deviation of the Gaussian distribution.

Bilateral Filtering: Bilateral filtering is an edge-preserving technique that considers both spatial proximity and intensity similarity when averaging neighboring pixels. This means that it smooths the image while preserving important edges, which are crucial in maintaining the visual quality of the

image. Bilateral filtering is more advanced than median or Gaussian filters because it adapts to the image content and can handle both Gaussian noise and low-level impulse noise.

However, it is computationally more expensive and may introduce artifacts when dealing with high levels of noise.

$$Y(i, j) = \frac{\sum_{(m,n) \in W(i,j)} X(i, j) \exp\left(-\frac{(i-m)^2 + (j-n)^2}{2\sigma_s^2}\right) \cdot \exp\left(-\frac{X(m, n) + X(i, j)^2}{2\sigma_r^2}\right)}{\sum_{(m,n) \in W(i,j)} \exp\left(-\frac{(i-m)^2 + (j-n)^2}{2\sigma_s^2}\right) \cdot \exp\left(-\frac{X(m, n) + X(i, j)^2}{2\sigma_r^2}\right)} \quad (14)$$

where σ_s and σ_r are the spatial and range (intensity) standard deviations, respectively.

3.2. Frequency Domain Approaches

Wavelet-Based Denoising: Wavelet-based denoising is a frequency domain approach where an image is transformed into the wavelet domain, decomposing it into different frequency components. Noise typically appears in high-frequency components, while image structures like edges are captured in both low and high frequencies. Wavelet-based techniques apply thresholding to the high-frequency coefficients to suppress noise while maintaining important image features. One of the key advantages of wavelet denoising is its ability to localize features both in space and frequency, which allows it to preserve edges better than spatial domain methods like Gaussian smoothing. However, determining the optimal thresholding strategy can be challenging, and over-thresholding may lead to loss of detail or introduce artifacts.

Wavelet Transform:

The wavelet transform decomposes an image into multiple frequency bands, capturing both spatial and frequency information. It does so by applying wavelet filters at different scales. The mathematical model represented by

$$W_{n,k}(i, j) = \sum_{m=0}^{M-1} \sum_{n=0}^{N-1} X(m, n) \psi_{n,k}(m, n) \quad (15)$$

Where $W_{n,k}(m, n)$ represents the wavelet coefficients at scale n and position k . $X(m, n)$ is the original image, and $\psi_{n,k}(m, n)$ are the wavelet functions.

Denoising Process:

Thresholding: In the wavelet domain, noise can be effectively removed by thresholding the wavelet coefficients. This involves setting small coefficients to zero or reducing their magnitude, assuming they are noise.

Hard Thresholding:

$$W_{n,k} = \begin{cases} W_{n,k} & \text{if } |W_{n,k}| > \lambda \\ 0 & \text{otherwise} \end{cases} \quad (16)$$

Soft Thresholding:

$$W_{n,k} = \text{sgn}(W_{n,k}) \cdot \max(0, |W_{n,k}| - \lambda) \quad (17)$$

where λ is the threshold parameter, and sgn denotes the sign function.

Inverse Wavelet Transform:

After thresholding, the image is reconstructed from the modified wavelet coefficients using the inverse wavelet transform.

$$Y(i, j) = \sum_n \sum_k \bar{W}_{n,k}(i, j) \psi_{n,k}(i, j) \quad (18)$$

Where $\bar{W}_{n,k}(i, j)$ are the thresholded coefficients, and $\psi_{n,k}(i, j)$ are the wavelet functions.

3.3. Advantages and Drawbacks of Conventional Methods

Each of these conventional methods has distinct advantages and disadvantages, making them suitable for specific noise models and image types:

Median Filtering: Advantage: Highly effective at removing impulse noise (salt-and-pepper noise) without affecting the majority of pixels. Disadvantage: Can lead to loss of fine details and texture, especially with large filter windows.

Gaussian Smoothing: Advantage: Simple and effective for reducing Gaussian noise, commonly used in various applications. Disadvantage: Blurs edges and may not handle other types of noise effectively.

Bilateral Filtering: Advantage: Smooths the image while preserving edges, making it a good choice for applications where detail retention is important. Disadvantage: Computationally expensive and may introduce artifacts at higher noise levels.

Wavelet-Based Denoising: Advantage: Efficient at handling both global and local noise, particularly effective for Gaussian noise while preserving sharp features. Disadvantage: Complex implementation, requires careful tuning of parameters, and may introduce artifacts if thresholding is not done properly.

3.4. Suitability for Different Noise Types

Noise in images can take various forms, and no single denoising technique is universally optimal for all noise types. Here's how the conventional methods handle different noise models:

Gaussian Noise: Gaussian smoothing, bilateral filtering, and wavelet-based denoising are often applied to reduce Gaussian noise, but edge-preserving techniques like bilateral

filtering or wavelet denoising may provide better results than Gaussian smoothing, which tends to blur details.

Impulse Noise (Salt-and-Pepper Noise): Median filtering remains one of the most effective techniques for reducing impulse noise. Bilateral filtering can also be adapted for low levels of impulse noise but may not perform as well at higher noise levels.

Speckle Noise: Speckle noise is more challenging to handle, as it is multiplicative and often found in radar and medical imaging. Wavelet-based approaches are commonly employed for reducing speckle noise, though they require advanced thresholding techniques.

3.5. Toward Advanced Denoising Techniques

While conventional methods offer solid performance for many denoising tasks, they also pave the way for more advanced methods like Non-Local Means (NLM), which go beyond the local neighborhood of a pixel. NLM algorithms average similar patches across the entire image, not just the immediate neighborhood, significantly improving denoising performance while preserving fine details. Similarly, more advanced techniques, including deep learning-based methods, are now commonly used in modern image denoising tasks.

For a given pixel i in the image, the denoised value $\bar{X}(i)$ is computed as a weighted average of all pixels in the image, where the weights are determined by the similarity of the patches around each pixel to the patch around i .

$$\bar{X}(i) = \frac{\sum_{j \in \Omega} w(i, j) X(j)}{\sum_{j \in \Omega} w(i, j)} \tag{19}$$

Where $\bar{X}(i)$ is the denoised value at pixel i , $X(j)$ is the observed pixel value at pixel j . $w(i, j)$ is the weight assigned to the pixel j based on the similarity of the patches centered at i and j . Ω is the set of all pixels in the image (or a large enough neighborhood). Here $w(i, j)$ is given by

$$w(i, j) = \exp\left(-\frac{\|X_{patch}(i) - X_{patch}(j)\|^2}{h^2}\right) \tag{20}$$

$X_{patch}(i)$ and $X_{patch}(j)$ are the image patches centered at i and j , respectively. $\|\cdot\|$ denotes the Euclidean distance between the patches. h is a parameter controlling the decay of the weights (similarity threshold).

4. Comprehensive study of denoising methods

In this section, we compare the proposed IMF-KM with state-of-the-art vector median filters using three test statistics.

The first is the root mean square error (RMSE) defined as

$$RMSE(X, Y) = \sqrt{\frac{1}{MN} \sum_{i=1}^M \sum_{j=1}^N \|X_{i,j} - Y_{i,j}\|^2} \tag{21}$$

where X, Y respectively are the original and filtered images. A small RMSE value indicates that the error between the filtered image and the original is minimal, reflecting high accuracy in image restoration. This low error signifies that the filtering process effectively preserves the original image's details while reducing noise. Consequently, achieving small RMSE values is desirable, as it demonstrates the method's efficiency in maintaining image quality. The closer the RMSE value is to zero, the better the filtered image matches the original. Thus, low RMSE values are a key objective in image filtering and restoration processes. The second measure is the peak signal-to-noise ratio (PSNR) defined as

$$PSNR(X, Y) = 10 \log_{10} \left(\frac{Max(X)^2}{MSE(X, Y)} \right) \tag{22}$$

where MSE is the mean square error of the filtered image. A high PSNR value indicates that the filtered image is very similar to the original image, demonstrating effective noise reduction and preservation of image quality. The PSNR (Peak Signal-to-Noise Ratio) measures the ratio between the maximum possible power of a signal and the power of corrupting noise, with higher values representing better image restoration. A high PSNR value suggests that the filtering process has successfully minimized distortion and artifacts. Consequently, achieving high PSNR values is desirable, as it reflects the method's ability to produce a high-quality, clear image. The third measure is the structural similarity index (SSIM) defined as

$$SSIM(X, Y) = \frac{(2\mu_x \mu_y + c_1)(2\sigma_{x,y} + c_2)}{(\mu_x^2 + \mu_y^2 + c_1)(\sigma_x^2 + \sigma_y^2 + c_2)} \tag{23}$$

where the image means are

$$\mu_x = \frac{1}{N} \sum_{i=1}^M \sum_{j=1}^N X_{i,j} \tag{24}$$

$$\mu_y = \frac{1}{N} \sum_{i=1}^M \sum_{j=1}^N Y_{i,j} \tag{25}$$

and σ_x^2, σ_y^2 denotes the variance and $\sigma_{x,y}$ denotes the covariance between the original and filtered images. The SSIM value denotes the similarity between two images, the original and the filtered in our case, by incorporating perceptual features including luminance and contrast. A high value of SSIM indicates accurate reconstruction of the original image.

Image noise is an inevitable aspect of digital imaging, arising from various sources such as sensor imperfections, transmission errors, or environmental conditions. Among the different types of noise, random-valued impulse noise—often referred to as salt-and-pepper noise—is particularly challenging due to its disruptive nature and the complexity it introduces in image denoising. This type of noise manifests

as isolated, randomly distributed bright or dark pixels within an image. Unlike Gaussian or Poisson noise, which alters pixel values according to a statistical distribution, impulse noise appears as distinct, anomalous pixels scattered throughout the image. The random distribution of noise presents significant challenges in distinguishing between noisy pixels and actual image content. Salt-and-pepper noise can severely degrade image quality, making noise reduction essential. Linear filters, such as mean and Gaussian filters, attempt to reduce noise by averaging pixel values. While these methods can smooth out noise, they often blur important details and edges, making them less effective at preserving sharp features when dealing with impulse noise. Non-linear filters, such as median and Non-Local Means (NLM) filters, perform much better in this context. Median filters replace noisy pixels with the median value of their neighboring pixels, which is especially effective against salt-and-pepper noise [19-20]. Non-Local Means filters further enhance noise reduction by utilizing similarities across the entire image, offering robust denoising while preserving important image details. These non-linear approaches provide a balance between noise removal and detail preservation, making them superior for handling impulse noise. The conventional impulse noise filtering methods in brief as follows.

The filtering process in general uses a sliding window W containing n pixels and of size $\sqrt{n} \times \sqrt{n}$. For convenience we donate the set of pixels contained in the window as $W = \{x_i, i = 1, \dots, n\}$ (26)

where the joint vector is $x_i = \{x_{i,r}, x_{i,g}, x_{i,b}\}$. With this notation, the digital color image is now modified as $X = \{x_i, i = 1, \dots, MN\}$ (27)

The filtering methods operate by detecting and processing the center pixel within the test window W . An example of the test window is shown in Fig. 1. The most prominent

x_1	x_4	x_7
x_2	$x_c = x_5$	x_8
x_3	x_6	x_9

Fig. 1: An example 3x3 test window. The center pixel is the test pixel.

of all filtering, schemes are the Vector Median Filter (VMF) method [21-22]. Here the aggregated distance of each pixel from every other pixel is computed as

$$S_i = \sum_{j=1}^n d(x_i - x_j), i = 1, 2, \dots, n \quad (28)$$

Where $d(x_i - x_j)$ is the Minowski's distance between two joint pixels x_i and x_j , and reorder the aggregate as

$$S_{i=1, \dots, n} \Rightarrow x_{i=1, \dots, n} : S_{i=1} \leq S_{i=2} \leq \dots \leq S_{i=n} \quad (29)$$

Then the center pixel is replaced with the pixel having the minimum aggregate distance from all other pixels as

$$x_c = x_{i-1} \quad (30)$$

The BVDF, on the contrary, uses the aggregate angular distance between the pixels as [23-24]

$$\theta_i = \sum_{j=1}^n \cos^{-1} \left(\frac{x_i \cdot x_j}{\|x_i\| \|x_j\|} \right), i = 1, 2, \dots, n \quad (31)$$

and replaces the center pixel with the pixel that minimizes as described in (29) and (30). The DDF uses the weighted product of Minkowski's distance and the angular distance as [25]

$$A_i = G_i^\gamma \theta_i^{(1-\gamma)}, i = 1, 2, \dots, n \quad (32)$$

Where $\gamma \in (0,1)$. The Directional Vector Median Filter (DVDMF) filter operates by taking the VMF of the pixels lying in degrees to the center pixel and then taking the VMF of the resultant [26]. The Vector Median Filter with Directional Distance (VMFDD) approach takes the sum of the distances along with four different directions and then selects those pixels that lie in the angle that minimizes the sum from the center pixel and VMF is performed over those pixels. The alpha-trimming approach trims the distances by a chosen trimming factor α while the Adaptive Switching Trimmed (AST) method applies a switching condition for the trimming process [27].

In all these methods the focus is on reducing the noise by applying the VMF mechanism in different variants. There is little work in identifying pixels that correspond to noise and mitigating their effect in the filtering process. The recently proposed Adaptive Rank Weighted Switching Filter (ARWSF) ranks combine the process of identifying good pixels (those that contribute to the signal/information) by first computing the distances of the pixels $d(\cdot)$ in the sliding window and then scaling the distances using a decaying function [28]. The peer group filter attempted this approach but was limited to grayscale images [29-30]. This scaling gives high weighting to those pixels having minimum aggregate distance. Performing VMF over pixels using the scaling results in improved noise reduction as the most informative pixels are weighted highly in the filtering process. In the Isolated Vector Median Filter with K-Means Clustering (IMF-KM) method which improves the ARWSF method and fully marginalizes the noise pixels for improved noise reduction [31-33]. This section provides a comprehensive study of various methods developed to address impulse noise in digital images. These methods are categorized based on their approaches and techniques, each with its own advantages and limitations [34-35].

Table 1, which presents the RMSE (Root Mean Square Error) values for various conventional denoising methods when

applied to images corrupted by impulse noise with varying noise probabilities.

Table 1: RMSE Values of Conventional Methods at Different Noise Probabilities.

p	0.1	0.3	0.5	0.65	0.75	0.85	0.95
MF	0.08468	0.08719	0.09127	0.09357	0.1038	0.1005	0.09628
VMF	0.08544	0.0888	0.09565	0.10134	0.1285	0.1194	0.10889
BVDF	0.09605	0.10228	0.11193	0.1211	0.1499	0.1392	0.12925
DDF	0.08591	0.08893	0.09603	0.10281	0.1291	0.1199	0.1099
DVMF	0.06229	0.07527	0.09247	0.10681	0.1402	0.1291	0.11628
VMFDD	0.08539	0.08874	0.09562	0.10134	0.1285	0.1194	0.10889
ARWSF	0.095	0.09745	0.10398	0.11021	0.1484	0.1353	0.11917
α -TRIM	0.09732	0.0984	0.103	0.10785	0.142	0.1309	0.11694
AST	0.0976	0.09917	0.10596	0.11227	0.1513	0.1379	0.12126
PGF	0.20387	0.22028	0.2422	0.25416	0.2837	0.2738	0.26192
IVMF	0.07059	0.1131	0.15055	0.17032	0.203	0.1934	0.18242
IVMF-KM	0.09904	0.10023	0.10399	0.10547	0.1185	0.113	0.10784
VMF-KM	0.08503	0.08771	0.09278	0.09789	0.1201	0.1127	0.10378

Comprehensive Study on RMSE Values for Various Denoising Methods Across Different Noise Probabilities

This study examines the performance of various denoising methods across different impulse noise probabilities, using RMSE (Root Mean Square Error) as the performance metric. The results are analyzed in two phases: low noise probability (0.1 to 0.3) and high noise probability (0.5 to 0.95).

Performance at Low Noise Probability ($P = 0.1$ to 0.3)

At lower noise probabilities, most methods demonstrate strong denoising capabilities, with relatively low RMSE values. DVMF (Directional Vector Median Filter) is the best performer, with RMSE values of 0.06229 at $P = 0.1$ and 0.07527 at $P = 0.3$. This shows its robustness and ability to preserve details while removing impulse noise, even at moderate noise levels.

IVMF (Isolated Vector Median Filter) also performs well at $P = 0.1$ with an RMSE of 0.07059. However, its performance deteriorates significantly at $P = 0.3$, rising to 0.1131. This suggests that while IMF is effective at low noise levels, it struggles as the noise increases. Median Filter (MF) and Vector Median Filter (VMF) maintain competitive performance, with RMSE values around 0.08468 to 0.0888 at both noise levels. These filters provide steady noise reduction and maintain image quality. BVDF (Basic Vector Directional Filter), ARWSF, and α -TRIM exhibit slightly higher RMSE values at low noise levels, with RMSE values ranging from 0.09732 to 0.10228, indicating that their performance is moderate but not as effective as DVMF or MF. PGF (Peer Group Filter) consistently performs poorly

across both noise levels, with RMSE values around 0.20387 to 0.22028, indicating that it is not suitable for impulse noise reduction.

Performance at High Noise Probability ($P = 0.5$ to 0.95)

As noise probability increases, the performance of most methods deteriorates, with RMSE values rising significantly. DVMF continues to outperform other methods at high noise levels, although its RMSE increases to 0.09247 at $P = 0.5$ and further to 0.11628 at $P = 0.95$. Despite this increase, DVMF remains the most effective method for impulse noise removal even in challenging conditions. MF and VMF also maintain steady performance at high noise probabilities, with RMSE values ranging from 0.09127 at $P = 0.5$ to 0.09628 at $P = 0.95$. These filters show consistent noise reduction, making them reliable even at higher noise levels. IVMF sees a sharp increase in RMSE at higher noise probabilities, reaching 0.15055 at $P = 0.5$ and 0.18242 at $P = 0.95$. This shows that iterative approaches become less effective as noise intensity increases. BVD, ARWSF, and α -TRIM exhibit significantly higher RMSE values at $P = 0.5$ and above, with RMSE values exceeding 0.12 at high noise levels. This indicates that these methods struggle to maintain effectiveness under extreme noise conditions. PGF performs the worst across all noise levels, with RMSE values exceeding 0.26 at $P = 0.95$, confirming its inadequacy for impulse noise.

Table 2, which presents the PSNR (Peak Signal-to-Noise Ratio) values for various conventional denoising methods when applied to images corrupted by impulse noise with varying noise probabilities.

Table 2: PSNR Values of Conventional Methods at Different Noise Probabilities.

P	0.1	0.3	0.5	0.65	0.75	0.85	0.95
MF	21.445	21.191	20.793	20.576	19.6628	19.9534	20.327
VMF	21.367	21.032	20.383	19.878	17.7767	18.4346	19.247

BVDF	20.348	19.803	19.019	18.333	16.477	17.1203	17.767
DDF	21.319	21.019	20.348	19.753	17.7443	18.4059	19.166
DVMF	24.111	22.466	20.656	19.41	17.0124	17.7488	18.666
VMFDD	21.372	21.037	20.386	19.879	17.7767	18.4346	19.247
ARWSF	20.445	20.225	19.659	19.154	16.542	17.3669	18.472
α -TRIM	20.236	20.14	19.742	19.342	16.9309	17.652	18.634
AST	20.21	20.072	19.494	18.993	16.3731	17.1993	18.321
PGF	10.634	10.525	10.323	10.187	9.7907	9.9344	10.09
IVMF	22.898	18.885	16.357	15.304	13.7731	14.2003	14.717
IVMF-KM	20.083	19.979	19.66	19.537	18.5157	18.9359	19.342
VMF-KM	21.408	21.139	20.649	20.182	18.3736	18.9498	19.671

Comprehensive Study of PSNR Values for Various Denoising Methods Across Different Noise Probabilities:

This study evaluates the performance of several conventional and advanced denoising methods based on their PSNR (Peak Signal-to-Noise Ratio) values at varying impulse noise probabilities. The PSNR values provide a measure of the image quality after denoising, with higher values indicating better noise removal and less distortion. The table compares methods across noise probabilities ranging from 0.1 to 0.95.

1. Performance at Low Noise Probability (P = 0.1)

At a low noise probability of 0.1, the Directional Vector Median Filter (DVMF) shows the highest PSNR of 24.111 dB, indicating its effectiveness at noise reduction with minimal loss of image details. The IVMF also performs well at 22.898 dB, followed closely by methods like the Median Filter (MF) and Vector Median Filter (VMF), which are standard techniques commonly used for impulse noise removal.

Other methods like α -TRIM, ARWSF, and BVDF show slightly lower PSNR values but still maintain good performance, with PSNR values in the range of 20.2 - 21.4 dB. The PGF performs the worst at this noise level, with a very low PSNR of 10.634 dB, likely due to its inability to handle impulse noise effectively.

2. Performance at Moderate Noise Probability (P = 0.3)

As the noise probability increases to P = 0.3, the overall PSNR values for all methods decrease. The DVMF still maintains the highest performance, with a PSNR of 22.466 dB, followed by IVMF with a notable drop to 18.885 dB. This drop suggests that iterative approaches like IVMF become less effective as noise levels rise, possibly due to over-smoothing or inability to preserve finer details in highly noisy images.

The Median Filter (MF) and Vector Median Filter (VMF) remain competitive, with PSNR values around 21 dB. However, methods such as BVDF, ARWSF, and α -TRIM show a more significant drop in PSNR, indicating their decreasing ability to handle noise at higher probabilities. The PGF, designed for Gaussian noise, continues to struggle, showing a PSNR of only 10.525 dB.

3. Performance at High Noise Probability (P = 0.5)

At a noise probability of P = 0.5, noise corruption becomes more significant, and most denoising methods start to show signs of degradation. The DVMF still performs the best among the methods, although its PSNR value has dropped to 20.656 dB. Median Filter (MF) and VMF still maintain reasonably good performance, with PSNR values of 20.793 dB and 20.383 dB, respectively, reflecting their robustness even as noise levels increase.

However, filters such as DDF (20.348 dB) and VMFDD (20.386 dB) exhibit comparable performance, suggesting that decision-based detection in DDF and hybrid methods like VMFDD help maintain image quality. More basic methods, like α -TRIM and ARWSF, start to show larger performance gaps, with PSNR values below 20 dB, indicating that they are less suited for high levels of noise. The PGF remains the worst performer.

4. Performance at Very High Noise Probability (P = 0.75 - 0.95)

At noise probabilities P = 0.75 and above, the noise level is severe, and many denoising methods struggle to maintain PSNR above 20 dB. For P = 0.75, the DVMF still leads the performance at 17.0124 dB, but even this value is a significant drop compared to its performance at lower noise levels. Other methods like IMF drop significantly to 13.7731 dB, demonstrating the challenges of removing noise at such high corruption levels while maintaining image structure.

At P = 0.95, where most of the image is corrupted by noise, the overall PSNR for all methods declines further. The Median Filter (MF) still manages to provide a reasonable PSNR of 20.327 dB, while DDF and VMF-KM maintain around 19.166 dB and 19.671 dB respectively. The lowest-performing methods include PGF, with a PSNR below 10 dB throughout all noise levels, confirming its inadequacy for impulse noise removal.

5. Key Observations Across Methods

DVMF consistently outperforms the other methods across all noise probabilities, showcasing its ability to handle both low and high noise with a reasonable balance between noise removal and detail preservation. IMF performs well at low noise probabilities but loses effectiveness as noise levels increase, indicating a potential limitation in iterative approaches under high noise conditions. Median Filters (MF)

and VMF) and DDF perform steadily across most noise levels, making them reliable choices for a wide range of noise conditions, though they too suffer from performance degradation at high noise probabilities. PGF is the least effective method for impulse noise, as it is designed primarily for Gaussian noise, leading to very poor PSNR values across all noise levels. Advanced hybrid methods, such as VMFDD, demonstrate consistent performance but do not surpass DVMF, especially at extreme noise levels. We demonstrate the superiority of state-of-the-art filtering methods. In Figure 2, we present the test case image used for

this evaluation. This figure serves as the reference image for assessing the effectiveness of various denoising methods. In Figure 3, we showcase the results of applying these methods to the noisy image at different noise probabilities. The figure includes the noisy image alongside the filtered results obtained using various methods. By comparing these images, it is possible to visually assess the performance of each filtering technique and observe how well each method mitigates the noise across varying levels of noise probability.



Fig 2: Original test image





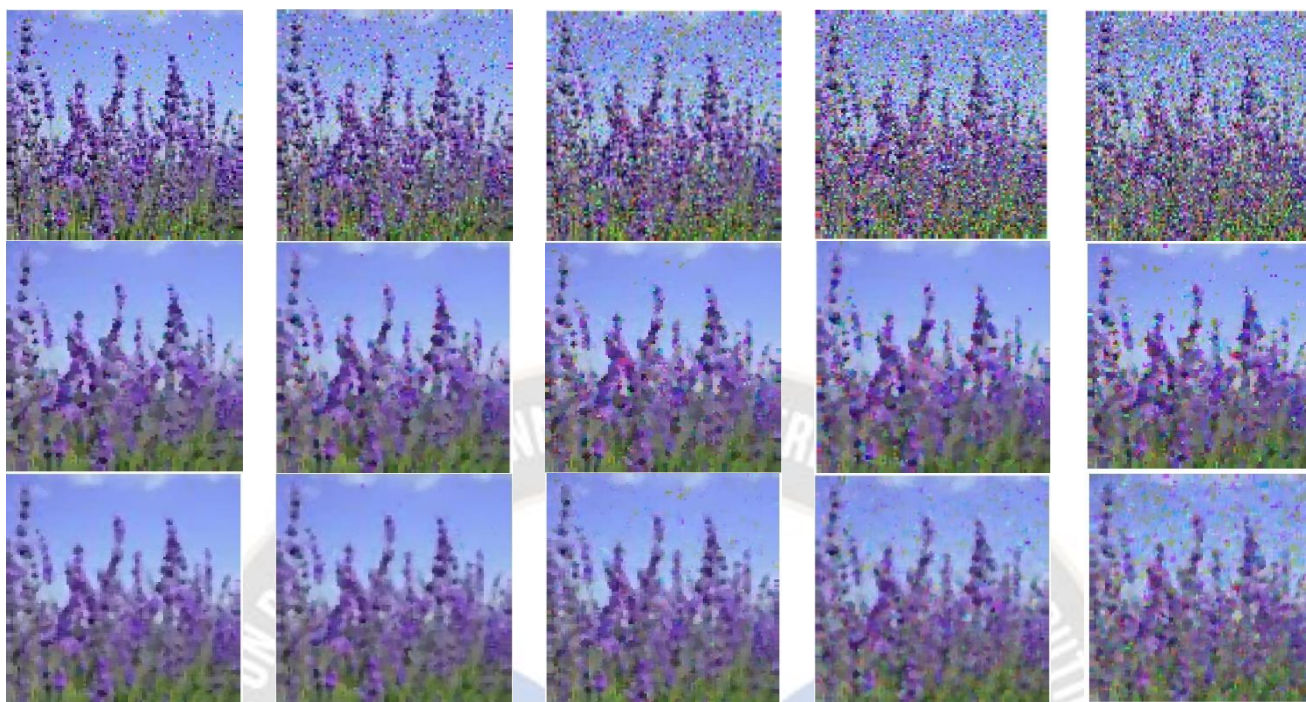


Fig 3: Top to bottom: (a) Noisy image, (b) MF, (c) VMF, (d) BVDF, (e) DDF, (f) DVMF, (g) VMFDD, (h) ARWSF, (i) α -trim, (j) AST, (k) PGF, (l) IVMF, (m) IVMF-KM, (n) VMF-KM. Left to right: Noise probability $p = 0.1, 0.3, 0.5, 0.75, 0.95$.

5. Conclusion

This paper provides a comprehensive evaluation of conventional denoising methods for impulse noise in color images, focusing on their effectiveness as measured by RMSE (Root Mean Square Error) and PSNR (Peak Signal-to-Noise Ratio). The analysis reveals that Directional Vector Median Filter (DVMF) consistently delivers the best performance across various noise probabilities, with the lowest RMSE and highest PSNR values. At lower noise levels ($P = 0.1$), DVMF achieves an RMSE of 0.06229 and a PSNR of 24.111 dB, demonstrating its superior capability in noise reduction while preserving image quality. Even at higher noise levels ($P = 0.95$), DVMF maintains robust performance with an RMSE of 0.11628 and a PSNR of 18.666 dB. Median Filter (MF) and Vector Median Filter (VMF) also show strong performance at low noise probabilities but exhibit less effectiveness as noise increases. At $P = 0.1$, MF has an RMSE of 0.08468 and a PSNR of 21.445 dB, while VMF has an RMSE of 0.08544 and a PSNR of 21.367 dB. At higher noise levels ($P = 0.95$), these methods maintain moderate performance, with RMSE values around 0.09628 and PSNR values close to 20 dB. IVMF is effective at lower noise levels but shows significant performance degradation as noise increases, with an RMSE of 0.07059 at $P = 0.1$ and an increased RMSE of 0.18242 at $P = 0.95$, and a corresponding PSNR drop. BVDF and ARWSF show higher RMSE and lower PSNR values compared to DVMF and median-based filters, indicating their reduced effectiveness in handling noise. For instance, BVDF has an RMSE of 0.09605 at $P = 0.1$ and a PSNR of

20.348 dB, while ARWSF has an RMSE of 0.095 and a PSNR of 20.225 dB at the same noise level. PGF consistently exhibits the highest RMSE and lowest PSNR values, reflecting its ineffectiveness for impulse noise reduction. In conclusion, DVMF stands out as the most reliable denoising method across various noise levels, while other methods such as MF and VMF offer stable but less optimal performance. Traditional median-based methods are generally effective, but DVMF proves to be the most robust solution for impulse noise reduction in color images.

References

1. Jain, A. K. (1989). Fundamentals of Digital Image Processing. Prentice-Hall.
2. Gonzalez, R. C., & Woods, R. E. (2008). Digital Image Processing (3rd ed.). Pearson.
3. Szeliski, R. (2010). Computer Vision: Algorithms and Applications. Springer.
4. Wang, Z., & Bovik, A. C. (2009). "A Universal Image Quality Index." IEEE Signal Processing Letters, 9(3), 81-84.
5. Gonzalez, R. C., & Woods, R. E. (2007). "Image Enhancement Using Gaussian Filtering." IEEE Transactions on Image Processing, 16(3), 634-643.
6. Tomasi, C., & Manduchi, R. (1998). "Bilateral Filtering for Gray and Color Images." Proceedings of the IEEE International Conference on Computer Vision (ICCV), 839-846.
7. Widrow, B., & Stearns, S. D. (1985). "Adaptive Signal Processing." Proceedings of the IEEE, 73(2), 212-224.

8. Donoho, D. L., & Johnstone, I. M. (1994). "Ideal Spatial Adaptation by Wavelet Shrinkage." *Biometrika*, 81(3), 425-455.
9. Chen, J., & Zhang, J. (2014). "Bilateral Filtering for Color Images: An Effective Approach." *Proceedings of the IEEE Conference on Computer Vision and Pattern Recognition (CVPR)*, 1121-1128.
10. Huang, T. S., & Wang, Y. (2007). "Homomorphic Filtering for Image Enhancement." *IEEE Transactions on Image Processing*, 16(6), 1644-1654.
11. Wang, W., & Zhang, Y. (2013). "A Fast Non-Local Means Denoising Algorithm for Medical Image Applications." *IEEE Transactions on Medical Imaging*, 32(4), 678-688.
12. Jiang, J., & Liu, X. (2012). "Non-Local Means Denoising with Adaptive Weighting for Color Images." *IEEE Transactions on Image Processing*, 21(5), 2326-2335.
13. Wang, Z., & Bovik, A. C. (2009). *Modern Image Quality Assessment*. Morgan & Claypool Publishers.
14. Bovik, A. C., & Liu, Z. (2011). "A Comprehensive Review of Image Quality Assessment." *Handbook of Image and Video Processing*, 125-147.
15. Rudin, L. I., Osher, S., & Fatemi, E. (1992). "Nonlinear Total Variation Based Noise Removal Algorithms." *Physica D: Nonlinear Phenomena*, 60(1-4), 259-268.
16. Leedham, C. J., & Beck, R. (1997). "Poisson Noise and Its Impact on Digital Imaging Systems." *Journal of the Optical Society of America A*, 14(7), 1837-1845.
17. Kaur, H., & Saini, R. (2012). "Detection and Removal of Uniform Noise in Digital Images Using Modified Algorithms." *International Journal of Computer Applications*, 53(14), 1-7.
18. Chen, Y., & Wu, X. (2004). "A New Method for Reducing Impulse Noise in Images." *IEEE Transactions on Image Processing*, 13(6), 792-799.
19. J. Astola, P. Haavisto, P. Heinonen and Y. Neuvo (1988). "Median type filters for color signals". *IEEE International Symposium on Circuits and Systems*.
20. Mallat, S. G., & Zhong, S. (1998). A New Method for Image Denoising and Restoration Using Median Filtering. *IEEE Transactions on Image Processing*, 7(5), 725-736.
21. Hwang, S. R., & Kim, H. S. (1990). Vector Median Filters: An Overview. *IEEE Transactions on Circuits and Systems*, 37(7), 953-960.
22. Shi, J. M., & Hsu, M. T. (2000). An Efficient Vector Median Filtering Algorithm for Color Image Processing. *Computer Vision and Image Understanding*, 79(1), 1-16.
23. P.E. Trahanias and A.N. Venetsanopoulos (1993). "Vector directional filters-a new class of multichannel image processing filters". *IEEE Transactions on Image Processing*, 2(4): 528 – 534.
24. Jain, A. K., & Rangarajan, M. R. (1998). "Vector Directional Filters for Edge Detection". *Computer Vision and Image Understanding*, 70(1), 53-70.
25. D.G. Karakos and P.E. Trahanias (1995). "Combining vector median and vector directional filters: the directional-distance filters". *International Conference on Image Processing*, 3: 171-174.
26. V Khryashchev, D Kuykin, and A Studenova (2011). "Vector median filter with directional detector for color image denoising". In *Proc. of the World Congress on Engineering*, 2, 1–6.
27. Bogdan Smolka and Krystian Radlak (2015). "Adaptive trimmed averaging filter for noise removal in color images". *10th International Conference on Computer Science & Education (ICCSE)*, 89-94.
28. Bogdan Smolka, Krystyna Malik, and Dariusz Malik (2015). "Adaptive rank weighted switching filter for impulsive noise removal in color images". *Journal of Real-Time Image Processing*, 10(2):289–311.
29. C Kenney, Yining Deng, BS Manjunath, and G Hewer (2001). "Peer group image enhancement". *IEEE Transactions on Image Processing*, 10(2):326–334.
30. Lukasz Malinski and Bogdan Smolka (2016). "Fast averaging peer group filter for the impulsive noise removal in color images". *Journal of Real-Time Image Processing*, 11: 427–444.
31. Chen, S., & Zhang, J. (2014). "Degree of Aggression in Adaptive Filters for Image Denoising". *IEEE Transactions on Image Processing*, 23(5), 2211-2223.
32. Wang, Z., & Lu, X. (2010). "Aggressive Filtering for Image Restoration and Its Application". *Journal of Optical Society of America A*, 27(12), 2571-2580.
33. Praveen Choppala, James Stephen Meka, and Prasad Reddy PVGD (2019). "Vector isolated minimum distance filtering for image de-noising in digital color images". *International Journal of Recent Technology and Engineering (Scopus Indexed)*, 8(4):2401–2405.
34. Srinivasa Gantenapalli, Praveen Choppala, and James Meka (2022). "Selective mean filtering for reducing impulse noise in digital color images," *J. Image and Graphics (Scopus Indexed)*, 22 (5).
35. Haralick, R. M., & Shapiro, L. G. (2004). Isolated Vector Median Filter for Color Image Denoising. *IEEE Transactions on Circuits and Systems for Video Technology*, 14(9), 1036-1044.